Anal. Chem. 2003, *75*, 1754–1764

A C_{60} Primary Ion Beam System for Time of Flight Secondary Ion Mass Spectrometry: Its Development and Secondary Ion Yield Characteristics

Daniel Weibel,[†] Steve Wong,[†] Nicholas Lockyer,[†] Paul Blenkinsopp,[‡] Rowland Hill,[‡] and John C. Vickerman*,[†]

Surface Analysis Research Centre, Department of Chemistry, UMIST, Manchester M60 1QD, U.K., and Ionoptika Ltd, Chilworth Science Park, Southampton SO16 7JF, U.K.

A buckminsterfullerene (C_{60})-based primary ion beam system has been developed for routine application in TOF-SIMS analysis of organic materials. The ion beam system is described, and its performance is characterized. Nanoamp beam currents of C_{60}^+ are obtainable in continuous current mode. C_{60}^{2+} can be obtained in pulsed mode. At 10 keV, the beam can be focused to less than 3 μm with 0.1 nA currents. TOF-SIMS studies of a series of molecular solids and a number of polymer systems in monolayer and thick film forms are reported. Very significant enhancement of secondary ion yields, particularly at higher mass, were observed using 10-keV C_{60}^+ for all samples other than PTFE, as compared to those observed from 10 keV Ga^+ primary ions. Three materials (PS2000, Irganox 1010, PET) were studied in detail to investigate primary ion-induced disappearance (damage) cross sections to determine the increase in secondary ion formation efficiency. The C_{60} disappearance cross sections observed from monolayer film PS2000 and self-supporting PET film are close to those observed from Ga^+. The resulting C_{60} efficiencies are 30–100 times those observed from gallium. The cross sections observed from C_{60} bombardment of multilayer molecular solids are ~100 times less, such that essentially zero damage sputtering is possible. The resulting efficiencies are >10^3 greater than from gallium. It is also shown that C_{60} primary ions do not generate any more low-mass fragments than any other ion beam system does. C_{60} is shown to be a very favorable ion beam system for TOF-SIMS, delivering high yield, close to 10% total yield, favoring high-mass ions, and on thick samples, offering the possibility of analysis well beyond the static limit.

Among the surface analysis techniques, the precise chemical specificity of static SIMS enables it to tackle many of the difficult problems thrown up by modern materials technology and the biosciences, for example, coatings on polymers, metals or textiles; biomolecules on cells or body tissue; toxic herbicides on foliage; synthesized molecules on combinatorial library beads, etc.[1-5] The incentive to achieve the best sensitivity is, therefore, enormous.

A good deal of research has been devoted to finding methods of improving the efficiency of ion formation and detection in static SIMS. The move from quadrupole to time-of-flight mass analyzers improved analysis sensitivities by 10^3 to 10^4.[7] It also dramatically increased the size (molecular mass) of species that could be detected and, thus, enabled materials of much greater chemical complexity to be analyzed. However, the yield of ions in the SIMS process is very low. From most materials, <1% of species sputtered from the surface are ionized.[6] Photo-ionization of the sputtered neutrals is proving to be an effective approach to increasing yields, and the area is the subject of active research in this laboratory and others.[8,10] In the area of compound analysis, laser desorption and MALDI have been rather successful in generating high yields of high mass molecular ions from large organic species.[11,12] However, sample consumption and contamination by the MALDI matrix mean that neither approach is applicable for true surface analysis at submicrometer spatial resolution. The basic requirement is to significantly increase the secondary ion yield (*yield*

* E-mail: John.Vickerman@umist.ac.uk.
† UMIST.
‡ Ionoptika Ltd.

(1) Vickerman, J. C. *Analyst* **1994**, *119*, 513.
(2) Benninghoven, A. *Angew. Chem. (Int. Ed. Engl.)* **1994**, *33*, 1023.
(3) Colliver, T. L.; Brummel, C. L.; Pacholski, M. L.; Swanek, F. D.; Ewing, A. G.; Winograd, N. *Anal. Chem.* **1997**, *69*, 2225.
(4) Brummel, C. L.; Vickerman, J. C.; Carr, S. A.; Hemling, M. E.; Roberts, G. D.; Johnson, W.; Weinstock, J.; Gaitanopoulos, D.; Benkovic, S. J.; Winograd, N. *Anal. Chem.* **1998**, *68*, 237.
(5) John, C. M.; Odom, R. W. *Int. J. Mass Spectrom. Ion Processes* **1997**, *161*, 47.
(6) *ToF–SIMS – Surface Analysis by Mass Spectrometry*; Vickerman, J. C., Briggs, D., Eds.; SurfaceSpectra and IM Publications: Manchester and Chichester, 2001.
(7) Tang, X.; Bevis, R.; Ens, W.; Lafortune, F.; Schueler, B.; Standing, K. G. *Int. J. Mass Spectrom. Ion Processes* **1988**, *85*, 43. Niehuis, E.; Heller, T.; Feld, F.; Benninghoven, A. *J. Vac. Sci. Technol.* **1987**, *A5*, 1243. Eccles, A. J.; Vickerman, J. C. *J. Vac. Sci. Technol.* **1988**, *A7*, 224.
(8) Benninghoven, A.; Hagenhoff, B.; Niehuis, E. *Anal. Chem.* **1993**, *65*, 630A.
(9) Brummel, C.; Willey, K. F.; Vickerman, J. C.; Winograd, N. *Int. J. Mass Spectrom. Ion Processes* **1995**, *143*, 257.
(10) Lockyer, N. P.; Vickerman, J. C. *Laser Chem.* **1997**, *17*, 139. Lockyer, N. P.; Vickerman, J. C. *Int. J. Mass Spectrom.* **2000**, *197*, 197.
(11) Hillenkamp, F.; Karas, M.; Beavis, R. C.; Chait, B. T. *Anal. Chem.* **1991**, *63*, 1193A.
(12) Menzel, C.; Berkenkamp, S.; Hillenkamp, F. *Rapid Commun. Mass Spectrom.* **1999**, *13*, 26.

10.1021/ac026338o CCC: $25.00
Published on Web 03/04/2003

2

being the number of secondary ions detected per primary ion impact), particularly of high mass "molecular" components from the surface of complex organic and inorganic materials while at the same time exercising more control over molecular fragmentation of species sputtered from molecular solids.

To date, the vast majority of static SIMS systems have used atomic primary projectiles; however, even in the early days of static SIMS, it was recognized that the higher mass Xe^+ (av m/z 131) beam generated a higher yield of ions to higher m/z than Ar^+ (m/z 40) of a similar energy.[13] Interest in the possible use of polyatomic primary species arose over 15 years ago. First, an $SF_6^{-/0}$ beam was developed, followed by ReO_4^- generated by heating a $Ba(ReO_4)_2$ ceramic[14] for use in quadrupole static SIMS systems. This was quite successful, with evidence that yields of molecular ions from a number of organic molecules—codeine, dopamine, etc.—could be increased over those observed for Cs^+ bombardment by 10−20 times.[15]

Recent experiments and molecular dynamics theory suggest that the efficient emission of large molecular species requires the correlated action of a number of cascades such that a number of soft impacts contribute to the "lift-off" of the molecule.[16] Atomic primary particles focus the energy deposition in a very small area, and there is evidence that a high proportion of the energy is deposited quite deep in the solid. The idea behind the application of a polyatomic primary particle is that while it would dissociate on collision with the surface, because of the spatial spread there would be the correlated impact of a number of atoms over a wider area — a splash effect.[17] MD simulations of 500 eV C_{60} sputtering from the surface of graphite has suggested that an acoustic wave is generated that essentially shakes molecules off the surface.[18] The effect is clearly specific to the layered character of graphite; however, the benefits of cooperative effects generated by large polyatomic projectiles are clear. Whatever the precise mechanism, the energy deposited per atom is lower, and hence, most of the energy will be deposited in the surface region. Thus, the use of polyatomic beams could be anticipated to give rise to higher yields of large molecules from the surface region.

In recent years, a number of groups have demonstrated increased secondary ion yield using a variety of polyatomic projectiles. The Münster group has exploited the use of SF_5^+ and shown that it can result in very significant increases in secondary ion yield, as compared to atomic projectiles, such as Ar^+, Xe^+, and Ga^+.[19] More significant was the fact that there were large increases in ion formation *efficiency* (defined as yield per unit of surface damage; see below). While the sputter rate and damage cross sections did increase, the secondary ion yield increase was very much greater.

It is the research carried out by groups in Texas and at Orsay in France into the enhancement of the secondary ion yield using gold cluster ions Au_n^+, as compared to ions formed from a number of large organic molecules, including C_{60} and $C_{24}H_{12}$ (coronene),[20,21,23] that has formed the principal stimulation for the present studies. Au_n^+ ions, where $n = 1-5$, from a heated gold source were shown to deliver strongly nonlinear increases in secondary ion yields from organic surfaces, such as phenylalanine or fatty acid LB films such that the yield of the $(M - H)^-$ per gold atom at the same energy per gold atom varied as 1:4:8:12 for $Au/Au_2/Au_3/Au_4$. This behavior was compared with sputter yields generated by large organic cluster ions, such as C_{60}^+ and $C_{24}H_{12}^+$ generated from a film of the organic materials (C_{60} or $C_{24}H_{12}$) using fission fragments from the decay of ^{252}Cf. The yield per unit mass of these ions was 4−5 times higher than for the gold projectiles of similar mass.[23] However, the nonlinear effect seen for gold is not observed for these large multiatomic particles; rather, the yield rises linearly with molecular mass. At a given total kinetic energy, the amount of energy deposited per volume unit in the solid appears to depend on the number of atoms in the projectiles. A TRIM calculation suggests that 20-keV C_{60} deposits most of its energy within 30 Å of the surface, whereas Au_4, which has a very similar mass, deposits its energy very much deeper in the solid, 115 Å. The shallow penetration depth and high secondary ion yield make these two ion systems very attractive as extremely surface sensitive high-yield primary projectiles for static SIMS analysis and molecular imaging. C_{60} provides the opportunity to investigate and optimize the effect of projectile energy (from a few electron-volts per carbon atom to hundreds of electron-volts per carbon atom) on the yield of molecular ions and their fragmentation. Gold polyatomic beams from a liquid metal source offer the possibility of optimizing yield with good spatial resolution. Preliminary reports have described our early results.[24,25] This paper describes in detail the development of a practical and robust C_{60} ion beam system and an investigation of its secondary ion yield characteristics from a range of inorganic and organic materials. A subsequent paper will describe a similar study of gold cluster ion beam system.[25]

DESIGN AND CONSTRUCTION OF THE C_{60} ION BEAM SYSTEM

The aim was to produce a practical and robust primary ion beam system based on C_{60} for incorporation on current and future TOF-SIMS systems. The design specification called for a primary ion energy range of 300−20 keV delivering ~1 nA continuous beam flux into a beam focus of <100 μm.

(13) Briggs, D.; Hearn, M. J. *Int. J. Mass Spectrom. Ion Processes* **1985**, *67*, 47.
(14) Appelhans, A. D.; Delmore, J. E.; Peterson, E. S. *Int. J. Mass Spectrom. Ion Processes* **1991**, *108*, 179. Ingram, J. C.; Croonewold, G. S.; Appelhans, A. D.; Delmore, J. E.; Dahl, D. A. *Anal. Chem.* **1995**, *67*, 187.
(15) Appelhans, A. D.; Delmore, J. E. *Anal. Chem.* **1989**, *61*, 1685; **1989**, *61*, 1687.
(16) Delcorte, A.; Bertrand, P.; Vickerman, J. C.; Garrison, B. J. In *Secondary Ion Mass Spectrometry, SIMS XII*; Benninghoven, A., Bertrand, P., Migeon, H.-N., Werner, H. W., Eds.; John Wiley & Sons: New York, 2000; p 27. Delcorte, A.; Garrison, B. J. *J. Phys. Chem. B* **2000**, *104*, 6785.
(17) Nguyen, T. C.; Ward, D. W.; Townes, J. A.; White, A. K.; Krantzman, K. D.; Garrison, B. J. *J. Phys. Chem. B* **2000**, *105*, 8221.
(18) Kerford, M.; Webb, R. P. *Nucl. Instrum. Methods Phys. Res., Sect. B* **2001**, *180*, 44.
(19) Kötter, F.; Benninghoven, A. *Appl. Surf. Sci.* **1998**, *133*, 47.
(20) Boussofiane-Baudin, K.; Bolbach, G.; Brunelle, A.; Della-Negra, S.; Håkansson, P.; Le Beyec, Y. *Nucl. Instrum. Methods* **1994**, *B88*, 160.
(21) Le Beyec, Y. *Int. J. Mass Spectrom.* **1998**, *174*, 101.
(22) Kaercher, R. G.; da Silveira, E. F.; Barros Leite, C. V.; Schweikert, E. A. *Nucl. Instrum. Methods* **1994**, *B94*, 207.
(23) Harris, R. D.; Van Stipdonk, M. J.; Schweikert, E. A. *Int. J. Mass Spectrom. Ion Processes* **1998**, *174*, 167. Harris, R. D.; Baker, W. S.; Van Stipdonk, M. J.; Crooks, R. M.; Schweikert, E. A. *Rapid Commun. Mass Spectrom.* **1999**, *13*, 1374.
(24) Wong, S. C. C.; Blenkinsopp, P.; Lockyer, N. P.; Weibel, D. E.; Vickerman, J. C. *Appl. Surf. Sci.* **2003**, *203*–*204*, 219.
(25) Davies, N.; Weibel, D. E.; Lockyer, N. P.; Blenkinsopp, P.; Hill, R.; Vickerman, J. C. *Appl. Surf. Sci.* **2003**, *203*–*204*, 223.
(26) Davies, N.; Weibel, D. E.; Lockyer, N. P.; Blenkinsopp, P.; Hill, R.; Vickerman, J. C. In preparation.

3

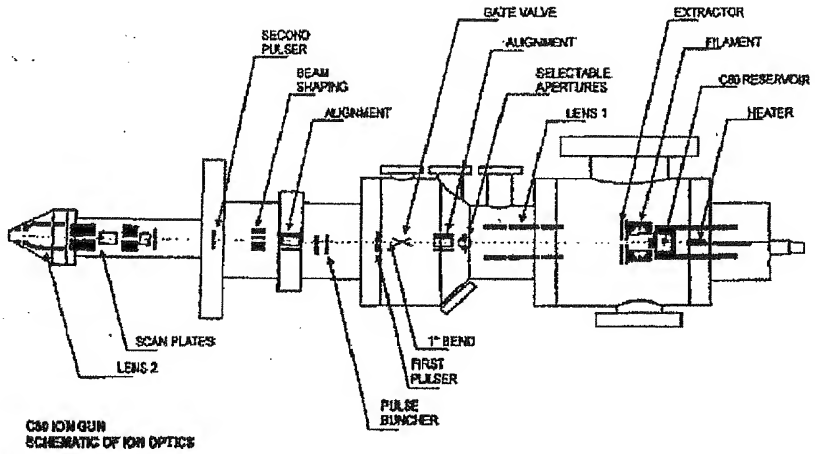

Figure 1. Schematic of C_{60} gun ion optics.

Source. Several source designs were considered: a plasma source, an thermal effusive source, and direct sputtering of the source materials by a small external ion beam. The final source design was based on the effusive source. It has proved to be simple to implement, and it has enabled the design specifications to be exceeded. A 0.5-g portion of C_{60} powder is heated at the rear of the source to a temperature of ~475 °C. C_{60} evaporates (~8 × 10^{-4} mbar) and is directed into the center of an ionization cell through a nozzle. A circular filament surrounds this cell, with a concentric cylindrical grid that accelerates electrons from the filament into the center of the source. The predominant ionization process resulting from collisions between low-energy electrons and C_{60} molecules is the formation of C_{60}^+, with lesser cross sections for multiply charged C_{60} ions and for positively charged fragments.[27] The lifetime of a C_{60} charge is in excess of 500 h.

Ion Optics. Following detailed ion optical modeling using 2D SIMION, the ion beam system shown in Figure 1 was constructed. Positive C_{60} ions are extracted from a fairly diffuse source region by a conical electrode and brought to a strongly demagnified field image just inside the extractor. The first lens then focuses the beam to an intermediate field image near the midpoint of the column. The beam is apertured for angular acceptance in this part of the column. A strongly demagnifying lens (lens 2) brings the beam to a final focus at the sample. The demagnifying nature of the optics means that a reasonably small spot size can be attained despite the relatively diffuse nature of the source. For operation at high spatial resolution, a lot of beam current is necessarily rejected within the column. However, the output from the source has proved sufficient to give a more than adequate beam for TOF-SIMS.

For TOF-SIMS analysis, it is necessary to chop the beam into short pulses, and the probe should not move across the sample at the beginning or end of the pulses. Lens 1 (Figure 1) focuses the ion beam to an intermediate field image between a pair of pulsing plates (first pulser). Lens 2 then transmits this intermediate image into the final focus on the sample. Hence, when the beam is deflected by these plates, there is no apparent change in the position of lens 2's object, and so no movement of the final image ("motionless blanking"). In reality, aberrations in the beam originating from the source geometry cause some movement or change in beam shape, but these effects are not severe in relation to the target spatial resolution of the system. It is desirable to eliminate any neutrals from the beam, because they will not be focused. This is achieved by a 1° bend in the optical column.

Mass Filtering. To obtain clean, short pulses of uniform intensity, the beam is mass-filtered using a double chopping system, sometimes known as a mass gate. Ions of different masses or charges in the beam travel down the column at different velocities. By placing a second pulser further down the column, operated at a controlled time delay after the first pulser, sections of the pulse corresponding to a particular mass range can be selected. The limitation of this technique is that the second pulser must operate in an interval between two discrete masses if "motionless" pulsing is to be preserved. The double chopping system installed in the column can separate C_{60}^+ from C_{60}^+ with pulses up to 150 ns, and C_{60}^{2+} from C_{60}^+ with pulses up to 600 ns. These figures apply when running the gun at 20 keV; longer pulses can be used with lower energies.

Double-Deflection Beam Scanning. A critical feature of the ion optics is that the second lens should be strongly demagnifying, and this means placing it as close to the sample as possible. Therefore, it was desirable to use double deflection before the lens, and this method of scanning is used in both *x* and *y*.

Other elements of the ion beam system shown in the schematic are (a) Two alignment units. These are quadrupole deflection plates used to bring the beam back on to the optical axis, compensating any drift off-axis in the extraction/lens 1 region. (b) Beam shaping. This is an octopole arrangement for optimizing the probe shape. (c) Pulse buncher. This is a chamber with front and rear electrodes. If a pulse is applied to the rear electrode as the beam pulse passes through the chamber, the beam pulse is compressed into a shorter time. This is used when high-mass

(27) Matt, M.; Dünser, B.; Lezius, M.; Deutsch, H.; Becker, K.; Stamatovic, A.; Scheier, P.; Märk, T. D. *J. Chem. Phys.* **1996**, *105*, 1880.

4

resolution analysis is required and when the primary ion beam pulse is the time reference for the TOF analyzer. (d) Selectable apertures. A selection of 5 removable apertures can be moved onto the optical axis to change the angular acceptance of the column. Thus, the column can run with high current and low spatial resolution, or lower current and high spatial resolution.

PERFORMANCE OF C_{60} SOURCE AND ION BEAM COLUMN

The C_{60} primary beam system was mounted on the BioTOF-SIMS system described elsewhere.[28] The axis of the primary ion gun is inclined at an angle of 50° to the target surface. Secondary ions are extracted into the TOF analyzer by biasing the sample stage ±2.5 keV relative to the extraction optics. All of the beam testing and spectral information was obtained using this analyzer. Although the ion beam system can be operated up to 25 keV, the studies reported here utilized a prototype power supply floating the source to 12.5 keV, which limited the beam impact energy to 10 keV in positive ion mode and 15 keV in negative ion mode. Secondary ion detection is by single ion counting via a 60:1 Galileo microchannel plate detector fitted with a facility to postaccelerate incoming ions up to 23 keV to enhance high-mass detection.

When the alignment of the source and lens voltages were optimized, an electron beam filament current of 1.8 A gave a maximum total target current of up to 2 nA of pure C_{60}^+ at 12.5 keV using the 1000-μm aperture. Raising the source heater temperature to 500 C increased the target current to 3 nA. The source grid voltage, which controls electron energy, influences both target current and beam composition. A grid voltage of 75 V delivers maximum total target current.

Beam composition can be estimated from the various contributions to a SIMS spectrum of a metal surface generated by an unfiltered primary ion beam. Varying the chopper delay times relative to the blanking voltage demonstrated that there are two principal contributions to the primary beam to be separated: C_{60}^{2+} (1.95-μs delay relative to the blanking pulse) and C_{60}^+ (2.75-μs delay). C_2 fragmentation of C_{60}^+ and C_{60}^{2+} ions makes a very minor contribution to the total beam at operational grid voltages, <0.5% at or below 45 V. C_2 losses do become more important at higher grid voltages, ~10% at ~70 V and 35% at 120V. By varying the grid voltage, the beam composition can be optimized. Measurements have shown that the secondary ion yield from C_{60}^{2+} bombardment is 2.4 times that from C_{60}^+ at the same beam acceleration potential (i.e., when the C_{60}^{2+} beam is twice the energy of the C_{60}^+ beam). Converting the observed absolute Al ion yield from Al foil as a measure of primary beam flux. Figure 2 plots the relative fluxes of C_{60}^+ and C_{60}^{2+} as a function of grid voltage.

Thus, a grid voltage of 25 V gives a relatively clean continuous C_{60}^+ beam. A 0.5–1-nA C_{60}^+ continuous current can be obtained through a 1000-μm aperture. This is stable within ~10% over a period of 8 h. As the C_{60} charge nears the end of its life, the beam current begins to decay, and this level of stability is lost. If the beam is mass-filtered using the beam chopper (or mass gate), maximum C_{60}^+ target currents can be achieved at 50 V grid voltage. At 75 V, we should expect some minor contribution of

(28) Braun, R. M.; Blenkinsopp, P.; Mullock, S. J.; Corlett, C.; Willey, K. F.; Vickerman, J. C.; Winograd, N. *Rapid Commun. Mass Spectrom.* **1998**, *12*, 1246.

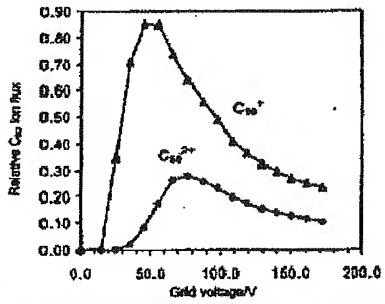

Figure 2. C_{60}^+ and C_{60}^{2+} primary ion flux relative to the maximum C_{60} ion flux as a function of ion source grid voltage.

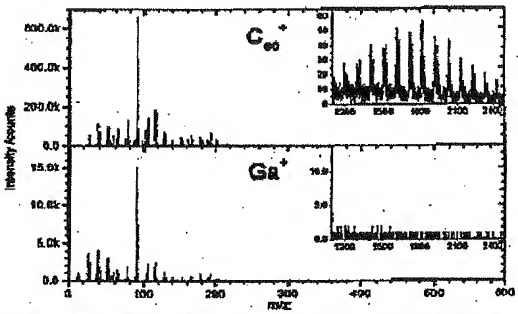

Figure 3. Positive TOF-SIMS spectrum of PS-2000 using 10-keV impact C_{60}^+ and Ga^+. Dose (ions): C_{60}^+, 4.05 × 10^6; Ga^+, 4.3 × 10^6.

smaller fullerene fragments. Nevertheless, they are efficiently filtered by the mass gate at 12.5 keV of energy. When C_{60}^{2+} is selected, the beam energy is effectively doubled. In most of the studies reported here, the ion beam was operated with a 40-ns pulse width and at 12.5 keV beam energy. This pulse width limits the mass resolution obtained in the present experiments to $m/\delta m$ ~ 750 at m/z 120; however, using the beam buncher, mass resolution in excess of 2000 can be obtained.

The ion optical design has enabled ~3-μm spatial resolution to be measured from a copper grid of 150 mesh, with the 100-μm beam forming aperture and 0.1-nA C_{60}^+ current. The 25-keV power supply should enable a smaller beam diameter to be attained (<1 μm). Thus, operationally, the ion beam system has more than met all of the design specifications.

RESULTS AND DISCUSSION

Inorganic Standards. The development of the new ion beam system was primarily directed toward increasing secondary ion yields particularly in the high-mass "molecular" region from organic and bio-organic materials. It is, however, conventional to quantify the performance of primary ion beams together with the analysis detection system using inorganic targets, such as aluminum and silicon. We have used aluminum, copper, silver, and gold foils. They were etched (100 × 100 μm) under a continuous 12.5-keV C_{60}^+ beam to various dose levels (10^{12} ions cm^{-2}, 10^{13} ions cm^{-2}; static limit, 10^{14} ions cm^{-2} and 10^{15} ions cm^{-2}) to monitor the spectral yield, the surface cleaning effects, the yield

of elemental ions per nC, and whether any carbon deposition occurred. For aluminum, the positive ion spectrum below the static limit shows evidence of surface hydrocarbon and $Al_2O_3nH_2O$ peaks characteristic of hydroxylated aluminum surfaces. Beyond the static limit, the hydrocarbons and hydroxides are removed. The surface is essentially "clean" metal after a dose of 10^{14} primary ions cm^{-2} (10 times the static limit). There is no evidence of any significant carbon deposition in the positive ion mode, and the yield is 2.5×10^8 counts $^{27}Al^+/nC$ using a 12.5-keV C_{60}^+ beam. This is of the same order as the standard accepted TOF-SIMS performance parameter using ~20-keV Ga^+ of 10^8 counts $^{27}Al^+/nC$ primary beam dose. The performance of the BioTOF-SIMS with 22 keV of postacceleration on the detector is $>5 \times 10^8$ counts $^{27}Al^+/nC$ using a 25-keV Ga^+ beam.

In the negative ion spectrum of aluminum, it is clear that in addition to residual AlO and AlO_2 signals, at high dose, $>10^{14}$ ions cm^{-2} signals are observed because of AlC_n, where $n = 2, 3, 4$ species, suggesting the formation of a surface carbide. On gold above 10^{14} ions cm^{-2}, signals due to C_n^- where $n = 2-16$ and AuC_n^- where $n = 2, 4, 6, 8$ are observed to grow. Similar behavior was observed on silver. On copper after 5×10^{15} ions cm^{-2} (or 500× the static limit), there was evidence of a weak C^+ signal and the growth of $Cu_3C_2^+$. Thus, C_{60}^+ is effective as a primary ion beam for surface cleaning; however, the deposition of carbon occurs at high ion doses. There is no evidence of C_{60} deposition at the energies used. At 10 keV impact, extensive fragmentation of the molecule is expected, although destruction into single carbon atoms may not be complete.[29]

In light of the subsequent results reported here, it is interesting that there is no real enhancement of secondary ion yield on sputtering metallic samples. The relative yield of metallic clusters M_n^+ appears to be somewhat different from those observed using other ion beams. These observations will be reported in more detail in a subsequent paper.[30]

Organic Materials. Two sets of materials that are generally accepted as representative of molecular solids and polymers have been studied.[31] The aim is to compare yield and fragmentation data under 12.5-keV Ga^+ and 12.5-keV C_{60}^+ ion bombardment: The molecular solids consist of a peptide, gramicidin D; an antioxidant, Irganox 1010; a lipid, dipalmitoyl phosphatylcholine, DPPC; γ-cyclodextrin (Cavamax W8); and a very low molecular weight polystyrene, PS-2000. The polymers consist of, poly(ethylene-terephthalate), PET; polystyrene, PS; and poly(tetrafluoroethylene), PTFE. Three types of sample were studied: thin sub-/monolayer films and thick multilayer films supported on silicon wafers or thick self-supporting films.

Spectra from Molecular Solids. The spectrum of PS2000 is typical of those obtained from the molecular solids and, indeed, the polymers. Figure 3 shows the positive ion spectra obtained at 10 keV impact energy for C_{60}^+ and Ga^+. Spectral acquisition took ~150 s for C_{60}^+. For all of the samples studied, a large increase in secondary ion yield is apparent using the C_{60}^+ primary ions, and this is especially evident in the higher mass region.

Spectra from Polymers. The same observations were obtained from the polymer materials. Again, there is a very considerable increase in yield such that the oligomer distribution is clearly observable from a polymer film when C_{60}^+ is used.

Yield Enhancement. In the following, the aim is to assess secondary ion yields generated by C_{60}^+ relative to other ion beams (mainly Ga^+) as applied in TOF-SIMS. We therefore use the measures of performance generally used in static SIMS research: yield, damage or disappearance cross section, and secondary ion formation efficiency. These are defined as they are used and are summarized very nicely by Kötter and Benninghoven in ref 19. The precise variation of secondary ion yield with mass observed will vary from instrument to instrument, depending among other things on ion optical configuration of the TOF-SIMS instrument and whether the detector is fitted with postacceleration facilities to enhance the detection of high mass (>500-Da) ions. At present, the only reliable way to compare relative performance of TOF-SIMS instruments is by obtaining data from identical samples on the instruments to be compared. Most of the data reported are from our BioTOF-SIMS, but we have compared performance with an IONTOF IV.

Table 1 summarizes the yield increases for a number of materials. The general conclusion is that under C_{60}^+ bombardment, *yields overall increase by in excess of 30 times. Some molecular ions can be detected only with* C_{60}. The yield enhancements vary across the mass scale, in the majority of cases increasing with mass. A curiosity is that although an enhancement is observed from PTFE, it is only between 2 and 10, much smaller than that observed from other materials. This agrees with a similar observation made by Benninghoven et al.[15] under SF_5^+ bombardment. At the time, it was thought that this lower enhancement might be due to the fact that fluorine formed part of the primary ion. This is clearly not the case. The mechanism of sputtering or secondary ion formation from PTFE must be different from other polymers.

In assessing the relative benefits of C_{60}^+ as a primary ion for TOF-SIMS, it is relevant to assess performance relative to other atomic and polyatomic ions. At present, the most widely used polyatomic ion in practical TOF-SIMS analysis is SF_5^+. We do not have an SF_5^+ beam line, so we are unable to make direct experimental comparison with C_{60}^+ performance within our own instrument. Comparison with SF_5^+ performance in an IONTOF instrument at the U.K. National Physical Laboratory has been possible, and this will be discussed later. However, as indicated earlier, we have also explored the performance of atomic gold and gold cluster ions.[28] Figure 4 compares the yields for PET. It can be seen that for the generation of large molecular ions, C_{60}^+ delivers the highest yield, even when compared to Au_3^+.

Although most of our studies have been limited to 12.5-keV primary beam energy (yielding impact energies of 10 keV for positive ions and 15 keV for negative ions), it has been possible to assess the effect of beam energy on yield in the range up to 30 keV by combining data obtained as a function of energy using both C_{60}^+ and C_{60}^{2+}. Figure 5 shows that the yield rises with primary ion energy in both the *m/z* 50–400 and the *m/z* 400–2500 ranges. However, the relative yields increase proportionately more in the high-mass region, suggesting that there are yield benefits to be gained by working at even higher primary energies.

(28) Beck, R. D.; Rokenberger, J.; Weis, P.; Kappes, M. M. *J. Chem. Phys* **1996**, *104*, 3638.
(30) Weibel, D.; Lockyer, N. P.; Vickerman, J. C. To be submitted to *J. Phys. Chem.*
(31) *The Static SIMS Library, Version 3*; Vickerman, J. C., Briggs, D., Henderson, A., Eds.; SurfaceSpectra Ltd.: Manchester, 2002.

Table 1. Absolute and Relative Secondary Ion Yields for Bulk and Spin-Coated Polymer Surfaces and Organic Compounds

compd	m/z	abs yield (Y × 10⁻³) C_{60}^-	abs yield (Y × 10⁻³) Ga^+	rel yield ($Y_{C_{60}^-}/Y_{Ga^+}$)
PET (bulk film), positive ions, 10.0 keV, C_{60}^- and Ga^-	10−50	3440	102	34
	50−100	5800	60.9	95
	100−200	3900	50.7	77
	200−400	806	12.9	62
	400−1000	223	3.77	59
	M + H	100	1.52	66
	2M + H	17.4	0.24	73
	3M + H	0.01	0.00	100
	4M + H	2.1	0.01	210
	9M + H	0.14		
	total	14 200	230	62
PS2000 (spin-coated monolayer), positive ions, 10.0 keV, C_{60}^+ and Ga^+	10−50	600	23.5	26
	50−100	2900	31	94
	100−200	3300	27.7	119
	200−400	900	5.2	173
	400−1000	100	0.3	333
	1350−2000	700		
	total	8000	87.9	91
PTFE (tape), positive ions, 10.0 keV, C_{60}^- and Ga^+	10−50	6500	1000	7
	50−100	3500	300	12
	100−200	2900	500	6
	200−400	170	50	3
	400−1000	27	12	2
	total	14 500	2160	7
Irganox 1010 (thick film), negative ions, 15.0 keV, C_{60}^+ and Ga^-	10−50	2300	70	33
	50−100	1300	6	217
	100−200	400	6	67
	200−400	300	6	50
	400−1000	160	20	8
	1000−2000	500		≥500
	molecular ion	2600		
	total	5000	130	38
Irganox 1010 (thick film), positive ions, 10.0 keV, C_{60}^+ and Ga^+	10−50	4018	25	159
	50−100	5745	26	219
	100−200	7296	37	195
	200−400	5513	44	126
	400−1000	746	6	133
	1000−2000	314	4	85
	total	23 629	142	166
Gramicidin D (thin spin-cast film), negative ions, 15.0 keV, C_{60}^+ and Ga^+	10−50	3200	67	48
	50−100	1000	37	27
	100−200	1000	38	26
	200−400	400	11	36
	400−1000	300	2.6	115
	1000−2500	80		
	molecular ion	300		
	total	6600	160	41
Cyclodextrin Cavamax W8 (thin spin-cast film), positive ions, 10.0 keV, C_{60}^+ and Ga^+	10−50	2306	74	31
	50−80	2527	86	29
	100−200	897	35	26
	200−400	202	8	26
	400−1000	110	5	21
	1000−1500	88	4	23
	molecular ion	24	1	24
	total	6129	212	29
DPPC (thin spin-cast film), positive ions, 10.0 keV, C_{60}^+ and Ga^-	10−50	16 990	454	37
	50−100	13 430	237	57
	100−200	4570	29	158
	200−400	600	8.7	69
	400−1000	144	1.7	85
	molecular ion	7.97	0.02	3985
	total	35 700	730	49

Careful examination of the energy-dependence data also suggests there may be a sputtering threshold at low primary energies. This will be examined in more detail elsewhere.[31]

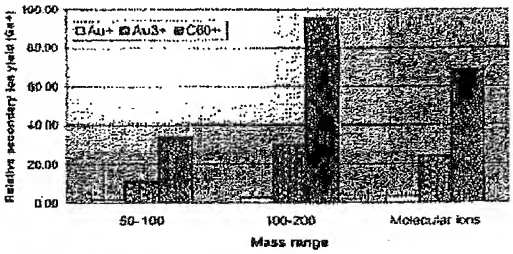

Figure 4. Comparison of positive secondary ion yields during analysis of PET using Au^+, Au_3^+, and C_{60}^+ primary ions at 10-keV impact energy.

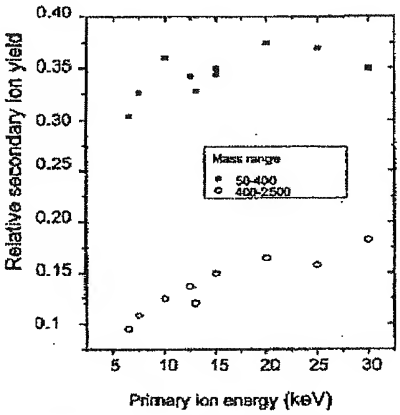

Figure 5. Relative secondary ion yield from gramicidin D with respect to total yield as a function of primary ion impact energy. Primary ions C_{60}^+ (6.5, 7.5, 10, 12.5, 15 keV) and C_{60}^{2+} (13, 15, 20, 25, 30 keV).

Relative Fragment Yield. Single event-by-event observations have suggested that there is an increase in low-mass fragment yield accompanying the overall increase in yield.[32] The implication is that the polyatomic primary ions break up the target molecular structure or impart more internal energy than atomic ions. However, this experiment examines the ion yield from discrete ion impacts on an essentially virgin surface. The fragment yields are the fragments produced from a single ion impact, as compared to the intact yield from a single impact. In general, fragment yields were significantly higher for single impacts of C_{60}, as compared to the atomic projectile, Cs. The ion yields here are the summation of many millions of events, giving a total ion dose of primary ions of 10^{13} to 10^{15}. Examination of the relative ion yields, $Y_{C_{60}}/Y_{Ga}$, as a function of mass for all the materials shows that there is no convincing evidence of a significant relative increase in low-mass fragment yield using C_{60} (see Figure 6 for gramicidin). The data in Figure 5 also suggest that relative fragment yield does not increase with energy.

(32) Diehnelt, C. W.; Van Stipdonk, M. J.; Schweikert, E. A. *Int. J. Mass Spectrom.* **2001**, *207*, 111.

7

Table 2. Yields ($Y(X^+)$), Disappearance Cross Sections ($\sigma(X^+)$), and Secondary Ion Formation Efficiencies ($E(X^+)$) for C_{60}^+ and Ga^+ Bombardment of PET, PS2000, and Irganox 1010

compound (positive ions, 10.0 keV, C_{60}^+ and Ga^+)	mass (u)	$Y(10^{-6})$		$\sigma(10^{-14}$ cm^2)		$E(10^8$ cm^{-2})		$N(X_i)$ from (100 nm)^2	
		Ga^+	C_{60}^+	Ga^+	C_{60}^+	Ga^+	C_{60}^+	Ga^+	C_{60}^+
PET (self-supporting thick film)	51	25	4270	0.63	1.85	40	2308	0.4	23
	104	98	5130	1.93	2.5	51	2052	0.5	21
	(M + H) 193	16	1000	2.74	4.76	6	210	0	2
	(2M + H) 385	2.5	174	5.1	5.9	0.5	29	0	0.3
	575	1	90	7.3	8.6	0.14	10	0	0.1
	769		21		10.8		2		0
	50−200	1116	92400	1.24	2.24	900	41250	9	412
PS2000 (spin-coated monolayer)	91	26	11000	0.55	0.22	47	6818	0.5	68
	178	10	900	1.77	1.17	6	769	0	8
	1200		74						
	50−200	467	59000	1.26	1.01	467	58416	5	584
PS2000 (thick multilayer film)	91	90	12000	1.85	0.04	49	300000	0.5	3000
	178	10	960	1.5	0.05	6.7	19200	0	192
	~1200		80						
	50−200	460	55800	1.17	0.04	393	1395000	4	14000
Irganox 1010 (thick multilayer film)	57	105	13300	2.20	0.081	48	164198	0.5	1642
	219	147	20500	3.9	0.093	38	220430	0.4	2204
	527	1.03	215	3.7	0.090	0.3	2389	0	24
	731	1.19	505	4.3	0.105	0.3	4810	0	48
	1176		237		0.14		1693		17
	51−215	637	130000	1.91	0.064	334	2031250	3	20312

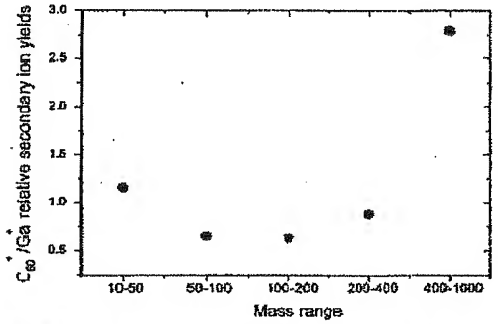

Figure 6. Relative ion yields in specific mass ranges observed using C_{60}^+ and Ga^+ primary ions from gramicidin D.

Disappearance (Damage) Cross Sections. While very considerable increases in ion yield have been observed using C_{60} primary ions, the most significant parameter is whether the ion yield relative to the amount of material removed from the surface has increased. To seek to measure this, the parameter efficiency, being the ion yield relative to the disappearance cross section, has been defined.[19] The disappearance cross section, σ, is frequently measured by following the decrease of mass spectral peaks, which are thought to be a measure of the surface concentration of the chemistry being studied. Peaks that have a clear structural relationship to the material being sputtered are generally chosen. However, it is important to note that the decay of such a peak can imply either (or both) the actual removal of the compound from the surface by sputtering or the destruction of the chemical structure by the bombardment process (hence, the parameter is sometimes referred to as the *damage* cross section). Using this approach, σ has been measured for a number of materials: gramicidin, Irganox 1010, PET, and PS2000. The experiment entails systematically monitoring the decrease in ion yields as a function of ion dose up to and beyond the static limit, 10^{13} primary impacts cm^{-2}. The full details of these experiments will be reported elsewhere as part of an investigation of the mechanism of sputtering of organic materials by C_{60}.[30] For the purposes of this paper, Figure 7 illustrates the data obtained from the low-molecular-weight polymer PS2000. Data from monolayer (A) and thick multilayer films (B) under C_{60}^+ bombardment are presented.

It can be seen that other than the signal at m/z 28 due to the silicon substrate, all of the ion signals from the thin film sample decay exponentially with ion dose in a manner observed for many primary ion/materials systems. The resulting cross sections observed from Ga^+ or C_{60}^+ bombardment of thin film organics and high-molecular-weight polymers are very similar within a factor of ~2 in the range $1-6 \times 10^{-14}$ cm^2 (Table 2). However, the signal decay from the multilayer film is very much slower: indeed, within the fluence region, ~$1-50 \times 10^{13}$ primary impacts, the signals are almost constant. Consequently, $\sigma_{PS2000} \sim 0.03 \times 10^{-14}$ cm^2. A similar value has been obtained for thick film Irganox 1010. These cross sections imply that very little chemical damage is being generated. Clearly, material is being removed, because for PS2000, it can be seen that beyond 60×10^{13} impacts, m/z 28 from the silicon substrate starts to rise. However, the sputtering process is not generating significant chemical structure damage. This suggests that some organic materials may be sputtered using polyatomics with minimal chemical damage. In principle, this should enable chemical depth profiling of such materials. Gillen and co-workers have reported similar observations with SF_5^+ and C_n^- ($n = 6-10$) bombardment of glutamate and acetylcoline and PMMA.[33-35] When the interface with the substrate aluminum or silicon is approached (as evidenced by an increase in the substrate

(33) Gillen, G.; Roberson, S. *Rapid Commun. Mass Spectrom.* **1998**, *12*, 1303.

8

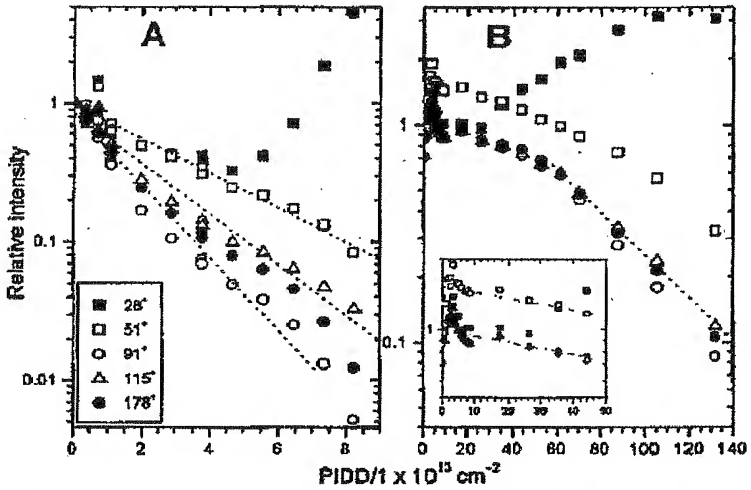

Figure 7. Relative yield of characteristic positive fragment ion intensities as a function of primary ion dose density obtained from (a) a thin approximately monolayer film of PS-2000 spin-cast on a silicon wafer under 10-keV C_{60}^+ bombardment and (b) a thick multilayer film of PS-2000 under 10-keV C_{60}^+ bombardment.

secondary ion signal), the disappearance rates do increase significantly. In contrast, the disappearance cross sections observed for C_{60} sputtering of a thick self-supporting films of high-molecular-weight PET are not low and are similar to those due to gallium sputtering. The reasons for the variation in disappearance cross section using C_{60} will be considered elsewhere; however, these data allow us to compute the yield efficiencies. These are also tabulated in Table 2. In all cases, C_{60} delivers very considerable increases in efficiency, but the increases are particularly large for the thick samples of PS2000 and Irganox where the disappearance cross sections are very low. However, in these latter cases, because the films of material are thick, the ion yields are actually being measured relative to the *degree of chemical structural damage generated*, NOT the amount of material removed. An external measure of material removed would be required to get a strict measure of efficiency. However, the reported parameter does suggest that for some materials, analysis of thick samples using C_{60}^+ primary ions does not need to be limited by the static limit. The high efficiencies imply that high yields can be obtained from chemically relatively undamaged surfaces through the use of high primary ion fluence levels.

ASSESSMENT OF THE C_{60} ION BEAM SYSTEM FOR TOF-SIMS

One of the primary aims behind the development of the C_{60} ion beam system was to radically increase the ion yield efficiency to enable TOF-SIMS analysis of bio-organic systems with good spatial resolution. In a 500- × 500-nm pixel area, there are only ~10^6 molecules. Conventionally, since SIMS is destructive, it is necessary to maintain the ion beam fluence well below 10^{13} primary impacts to ensure that static conditions apply; i.e., that no more than 1% of a monolayer is removed, and that minimal chemical damage occurs. The ion yield is usually $<10^{-3}$; consequently, there will be fewer than 10 ions detectable per pixel, far too few for an informative mass spectrum! Since the transmission of modern TOF-SIMS instruments is close to optimum, the only means of increasing the signal intensity is by increasing the ion yield by around 2 orders or relaxing the static limit requirement. The studies reported here demonstrate that a C_{60} -based ion beam system enables both aims to be attained for a number of important classes of organic and bio-organic materials without concomitant increases in low-mass fragment yield. From most materials, other than PTFE, total secondary ion yields are 1−2 orders higher than those observed with gallium. Total yields with 10-keV C_{60} are in the region of the required 10% or more. Furthermore, for some thick film materials, the disappearance cross sections are close to zero, such that ion yield efficiencies compared to gallium are 10^5 times higher. For such materials, it would appear that the static primary dose limit could be ignored, providing even higher yields. The benefits of this for high spatial resolution analysis are highlighted as follows: The total number of ions $N(X_i)$ that can be generated from a given sample area, A, can be simply calculated as EA. Reference to the final column of Table 2 shows that using C_{60}, the higher efficiencies would in principle enable informative spatially resolved analysis at least to the 100- × 100-nm pixel level. The data suggest that combining groups of characteristic peaks over a range of m/z should allow analysis at this resolution down to the 1% level for multilayers of some molecular solids.

Even where disappearance cross sections are more akin to those obtained with other atomic ions, from thin films or PET films, C_{60} yield efficiencies are still 10−10^2 times higher, and relative efficiency increases with mass. In these cases, while

(34) Piwon, E. R.; Gillen, G.; Wijesundara, M. B. J.; Wallace, W. E.; Hanley, L. *J. Phys. Chem. B* **2001**, *105*, 3950.
(35) Gillen, G.; King, K.; Freibaum, B.; Lareau, R.; Bennett, J.; Chmara, F. *J. Vac. Sci. Technol., A* **2001**, *19*, 568.

9

Table 2. Yields ($Y(X^+)$), Disappearance Cross Sections ($\sigma(X^+)$), and Secondary Ions Formation Efficiencies ($E(X^+)$) for Ga^+, Au^+, SF_5^+, and C_{60}^+ Bombardment of Thin Film PS2000

PS2000 (monolayer film)	primary ion	mass (u)						
		51	103	178	215	265	325	51–215
Y (10^{-6})	Ga^+, 10 keV	26	14	10	4	1		583
	Ga^+, 15 keV, IONTOF	24	13	9.3	2.8	0.7	0.2	555
	Au^+, 10 keV	39	62	49	20	5.6	1.7	2890
	SF_5^+, 10 keV, IONTOF	524	1550	1280	575	192	74	66300
	C_{60}^+, 10 keV	1500	1500	900	500	180	170	59300
σ (10^{-14} cm^2)	Ga^+	0.55	1.38	1.77	1.14	1.3		1.26
	Au^+	1.18	4.23	4.5	3.60	3.44	2.9	4.4
	SF_5^+ [a]	2.8	5.6	5.8	~6	~6	~6	5.8
	C_{60}^+	0.22	1.06	1.17	1.3	1.3	1.0	1.01
E (10^5 cm^{-2})	Ga^+, BioTOF	47	11	6	3.5	0.8		467
	Au^+	33	15	11	5.6	1.6	0.6	657
	SF_5^+, IONTOF	187	277	221	96	32	12	11431
	C_{60}^+, BioTOF	6818	1415	769	385	138	170	58713

[a] From ref 19.

analysis to 100 nm resolution might be possible in only very favorable cases, 500-nm resolution should be accessible. At present, the spatial resolution of the ion beam system is limited to 1 μm; however further development of the source and ion optics promise to deliver 100-nm resolution, which will enable the analyst to take full advantage of the analytical capability of the C_{60} ion beam. However, it is important to bear in mind that the present experiments have been limited to a 12.5-keV beam energy. If it is assumed that C_{60} completely dissociates, which as we have said is by no means certain at these energies, each impact carbon atom would have an energy of only 166 eV. The penetration depth will be minimal, a few angstroms. The energy dependence studies, Figure 5, show that the yields at least double at 20 keV and more than triple by 30 keV. Such an increase in primary energy that will be implemented with the updated power supply and will also improve the spatial resolution attainable by the present beam system. The C_{60} ion beam system therefore provides much of the radical improvement in secondary ion yield that is required to provide the sensitivity levels required, for example, for cellular imaging.

C_{60} SPUTTERING COMPARED TO OTHER POLYATOMICS

Our overall conclusion is that the C_{60} represents a considerable advance on atomic ion beam systems for TOF-SIMS. How does it compare with other polyatomic primary beams? As outlined in the Introduction, over the years, a number of different polyatomic ion beam systems have been studied; however, despite favorable results, most have not been put into routine use.

The gold cluster beams that the Orsay group investigated have been successfully developed further in our laboratory[25] and will be the subject of a subsequent paper.[26] The comparative data reported in Figure 4 shows that gold offers significant benefits for practical analysis. The yields observed with 10-keV Au_3^+ are not dramatically lower than with 10-keV C_{60}^+; however, such evidence as we have at present suggests that disappearance cross sections will be significantly greater than with C_{60}. Energy per impacting Au atom will be 3333 eV, so this is not surprising. However, as a liquid metal source, high spatial resolution will be much more easily attained, and it is expected in this laboratory to be the ion of choice for very high spatial resolution analysis.

The studies referred to above in which Gillen and co-workers studied the ion yields from films of tryptophan under 14-keV negative ion C_n^- bombardment on a Cameca IMS 4f instrument show a clear enhancement of $(M - H)^-$ yield by a factor ~10^3 between C_3 and C_{10}[25]. Tryptophan negative ion spectra are displayed for negative ion C_1, C_2, C_4, C_8, and C_{10} bombardment. It does seem that there may be a relative increase in low-mass fragmentation, although in the absence of quantitative data, it is not easy to be sure. Indeed, it is difficult to compare the overall yield and efficiency behavior with the present results, because useful yield data is not reported, and while it is clear from the glutamate film depth profile presented that low damage cross sections must apply, no quantitative data is provided.

While we do not have a SF_5^+ beam line, we have sought to compare the yield enhancements obtained in this work with C_{60}^+ with those obtained by the Münster group with 15-keV SF_5^+. It is difficult to make very accurate comparisons when the absolute detection efficiency of the two instruments used is not known and the beam energies used are different. The data reported in ref 19, in which the yields from polymer surfaces—PET, PS, PTFE, PC, PP, PEG, and PMMA—under Ar^+, Xe^+, and SF_5^+ bombardment did not report on gallium yields. We have therefore obtained yield information on our samples of PS2000 and PET from an IONTOF IV instrument at NPL using both gallium and SF_5^+. Table 3 reports the data and demonstrates that the absolute yields from PS2000 using 10-and 15-keV gallium are very closely similar using the two instruments. Thus, we can compare the yields obtained from PS2000 and PET with 15-keV SF_5 and 10-keV C_{60} with a reasonable degree of confidence. It seems that the yields are on a par. Clearly, the energy of the component atoms after fragmentation at impact will be very different. Their sputtering characteristics and, hence, their penetration depths will differ. After impact at 10 keV, assuming complete fragmentation of C_{60} (see proviso earlier), each carbon atom will have 166 eV of energy; the penetration depth will only be a few angstroms. However, in the case of 15-keV SF_5 the sulfur atom will have an energy of 3.8 keV and the fluorine atoms, 2.24 keV. They will therefore penetrate

10

well below the surface and into the substrate. The disappearance cross sections probably reflect the resulting subsurface damage. Whereas for thin film PS2000 using C_{60} the cross sections are around 1×10^{-14} cm², those for SF_5 as reported in ref 19 for polystyrene (molecular weight undefined) are around 6×10^{-16} cm². Consequently, the efficiencies for C_{60} are 5 times greater than for SF_5. However, as mentioned in the last section, it can be expected that yields with a 30-keV C_{60} beam should be at least 3 times greater than with the present 10-keV beam. The energy per carbon atom will still be only 500 eV, so disappearance cross sections should not be dramatically increased. Further efficiency increases should be possible.

Sputtering by C_{60}. There are two remarkable observations in regard to the sputtering of the organic materials by 10-keV C_{60}. The first is that on thin films and thick film PET, the disappearance cross sections are very similar to and rarely greater than for 10-keV gallium. The second is the very low signal decay observed for C_{60} sputtering of thick films of PS2000 (Figure 7) and Irganox.[30] The resulting cross sections are in the range $0.04-0.09 \times 10^{-14}$ cm^{-2}. Consequently, the efficiencies are further enhanced. While the SF_5^+ data already referred to demonstrate that in many cases, this ion generates more damage than atomic ions, Gillen et al. have reported that sputtering thin films of glutamate and acetylecholine as well as a sample of PMMA using 5-keV SF_5^+ can result in low-damage sputtering, enabling the material to be depth-profiled.[31,31] This phenomenon is clearly associated with the mechanisms of polyatomic sputtering. A consensus is emerging from the experimental and MD simulation studies that the efficient sputtering of large molecular ions and fragments by atomic primary ions is a consequence of the generation of a number of cascades within the substrate material that cooperate to deliver simultaneous upward impacts over a wide area, enabling the large species to move off into the vacuum. When an organic material is bombarded by an atomic projectile, there are a number of possible sputtering scenarios, not all favorable for the emission of the large molecular species we ideally seek. Delcorte et al.[16] have identified four, ranging from low action/low yield through low action/high yield, high action/low yield to high action/high yield. It is the high action/high yield events that are shown to be particularly favorable for the emission of large molecular entities. Overlapping subcascades are generated in the surface region, resulting a high energy density, leading to the simultaneous motion of a major fraction of the atoms in the excited volume. These studies have recently been extended to consider the effects when large organic structures are sputtered.[36] The simulation suggests that the initial interaction gives rise to atomic collision cascades, but there is then a transition to a molecular vibrational motion regime. This vibrational excitation sets up a collective molecular motion resulting in the emission of large polyatomic clusters. For emission to occur, the collective motion has to be upward. This collective motion will be greatly facilitated by polyatomic bombardment.[17] If we imagine that the C_{60} sphere initially impacts intact, since the diameter of the sphere is ~7 Å, the area of impact would ~40 Å², so the maximum energy density dissipated into the surface for a 10-keV impact would be ~250 eV/Å². 13 times less than for 10-keV Ga^+, which has a radius of ~1 Å, yielding an impact area of 3.1 Å² and, hence, an energy density of ~3226 eV/ Å². Suffice to say here that the lower impact energy of the fragmented components of the bombarding polyatomic means that energy is largely deposited in the surface region over an expanded area, as compared to an atomic ion. The excitation would be expected to be predominantly vibrational in the surface region, so most of the molecules and fragments emitted will be from the surface. Compared to high-energy atomic bombardment, there would be expected to be much less subsurface damage. If the process can lift off whole molecules or molecular fragments, polyatomic sputtering could be likened to progressive peeling of an onion, the subsurface being largely undamaged. Thus, in the case of PS2000 and Irganox, the materials are made up of molecules of 1200–2000 or 3000 Da. We have shown that C_{60} is able to lift off molecules of this size. Clearly, in the sputtering process, some of these molecules will be fragmented, but the basic building block of the material can be peeled off intact. However, C_{60} sputtering of thick-film PET does not show this behavior; disappearance cross sections are comparable with gallium. This is a very high molecular weight material. It is not possible to remove oligomers or fragments without multiple bond breaking; furthermore, the polymer chains are entangled. Sputtering will entail considerable structural disruption affecting, both surface and subsurface: thus, it is perhaps not surprising that disappearance cross sections are high. Our hypothesis is, therefore, that C_{60} sputtering of thick organic materials can be carried out with low levels of structural damage if the material is composed of small(ish) molecular units (less than a few kilodalton) held together by noncovalent forces. Materials composed of very large extended units, as in high-molecular-weight polymers, might be expected to be damaged at a much higher rate. We are in the process of exploring this hypothesis further, and this will be the subject of a subsequent paper.[30] Very recent work has shown that C_{60} sputtering of a thick film of PS100 000 does result in disappearance cross sections comparable to those observed from PET. This contrasts with the PS2000 data and would tend to support our hypothesis. Clearly, our conclusions so far seem to be partly in agreement and partly at variance with the observation of Gillen et al. using SF_5; however, much more work is required to probe the degree to which polyatomic sputtering of organic materials is specific to the physical state, the chemistry, and the identity of the primary ion.

CONCLUSIONS

A practical C_{60} ion beam system has been developed that delivers at least 1 nA of C_{60}^+ current at 10 keV into a 10-μm spot. The system is capable of sub-3-μm spatial resolution with 0.1-nA beam current. A C_{60} charge has a lifetime of >500 h.

C_{60}^+ bombardment of some representative organic materials results in yield enhancements of at least 30–100-fold, as compared to yields observed under Ga^+ bombardment at the same energy, with total ion yields in the region of 1–10%.

Disappearance (damage) cross sections under C_{60} bombardment are observed to be dependent on the chemistry and the physical state of the material. High-molecular-weight polymers and monolayer films of molecular solids are damaged at about the same rate as under Ga^+ bombardment. Thick films of molecular solids show extremely low levels of damage as if the molecules are being peeled off the surface, leaving very little subsurface damage. For such materials, the static limit could be abandoned.

(36) Delcorte, A.; Bertrand, P.; Garrison, B. J. *J. Phys. Chem.* 2001, *105*, 9474.

C_{60}^+ primary ion bombardment delivers no more molecular fragmentation than any other primary projectile used in SIMS. Indeed, in most cases studied here, there is less fragmentation and a very dramatic increase in "molecular" ion yield.

The overall yields efficiencies are 10^2–10^4 higher using C_{60}^+, as compared to atomic primary ions dependent on chemistry and physical state.

Taking the ion yield enhancements together with the possibility that the static limit requirement can be removed for many materials, C_{60} has the potential to deliver the performance required to make TOF-SIMS chemical characterization at the submicrometer-to-100-nm level a possibility.

ACKNOWLEDGMENT

The work reported here was funded by the U.K. Engineering and Physical Sciences Research Council (EPSRC). The authors are very grateful to Dr. Ian Gilmore of the U.K. National Physical Laboratory for the provision of analysis data on the PS2000 and PET samples using SF_5^+.

Received for review November 22, 2002. Accepted January 31, 2003.

AC026338O